 doi:10.20944/preprints202203.0389.v1

Article

Efficient Operations of Micro-Grids with Meshed Topology and Under Uncertainty through Exact Satisfaction of AC-PF, Droop Control and Tap-Changer Constraints

Mikhail A. Bragin [1,†,‡]*, Bing Yan [2,‡], Akash Kumar [2], Nanpeng Yu [3] and Peng Zhang [4]

1 University of Connecticut, mikhail.bragin@uconn.edu
2 Rochester Institute of Technology, bxyeee@rit.edu, ak2358@g.rit.edu
3 University of California, Riverside, nyu@ece.ucr.edu
4 Stony Brook University, P.Zhang@stonybrook.edu
* Correspondence: mikhail.bragin@uconn.edu
† Current address: 371 Fairfield Way, Storrs, CT 06269 USA
‡ These authors contributed equally to this work.

Abstract: Micro-grids' operations offer local reliability; in the event of faults or low voltage/frequency events on the utility side, micro-grids can disconnect from the main grid and operate autonomously while providing the continued supply of power to local customers. With the ever-increasing penetration of renewable generation, however, the operations of micro-grids become increasingly complicated because of the associated fluctuations of voltages. As a result, transformer taps are adjusted frequently, thereby leading to the fast degradation of expensive tap-changer transformers. In the islanding mode, the difficulties also come from the drop of voltage and frequency upon disconnecting from the main grid. To appropriately model the above, the nonlinear AC power flow constraints are necessary. Computationally, the discrete nature of tap-changer operations and the stochasticity caused by renewables add two layers of difficulty on top of a complicated AC-OPF problem. To resolve the above computational difficulties, the main principles of the recently-developed "l_1-proximal" Surrogate Lagrangian Relaxation are extended. Testing results based on 9-bus system demonstrate the efficiency of the method to obtain the exact feasible solutions for micro-grid operations thereby avoiding approximations inherent to existing methods, while demonstrating that through the optimization, 1. the number of tap changes is drastically reduced, and 2. the method is capable of handling networks with meshed topologies.

Keywords: Micro-grids; Droop Controls; Tap Changers; Islanded Mode; AC OPF; Lagrangian Relaxation; Renewable Generation; Markov Process; Mixed-Integer Nonlinear Programming

Citation: Bragin, M. A.; Yan, B.; Kumar, A.; Yu, N.; Zhang, P. Efficient Operations of Micro-Grids with Meshed Topology and Under Uncertainty through Exact Satisfaction of AC-PF, Droop Control and Tap-Changer Constraints . *Preprints* **2022**, *1*, 0. https://doi.org/

1. Introduction

As the name suggests, a *micro-grid* is a relatively small geographically localized electricity grid intended to provide uninterrupted service to local communities such as campuses, business centers, hospital complexes, and other critical infrastructure. To enable self-sufficiency to hedge against blackouts caused by natural disasters, micro-grids typically include generators, combined heat and power, and batteries. With the recent push for clean, green, and renewable energy, micro-grids may also include solar panels. Other grid devices may also include electric vehicle (EV) charging stations.

Under normal conditions, micro-grids are typically connected to the main grid (e.g., a power distribution system) and may exchange power. The normal operations, therefore, include the proactive power generation at the least cost in anticipation of the increase/decrease in customer demand as well as in anticipation of fluctuations of power generation from renewables. The intermittency of renewables can, however, lead to fluctuations of voltage, which may lead to frequent adjustments of taps within on-load tap changers thereby leading to fast degradation of expensive equipment and adversely impacting micro-grid economic viability. Stochasticity as well as the discrete nature of the underlying problem need to be explicitly captured to design the optimal (or near-optimal) control to ensure a low-cost power supply to local communities.

 doi:10.20944/preprints202203.0389.v1

Under faulty conditions or upon detection of low voltage/frequency on the main grid side, the interconnecting device such as a circuit breaker opens to switch the micro-grid to the *islanded* mode. In this mode, the micro-grid's goal is to serve the local loads by using locally available distributed energy resources. The micro-grid's operations are also complicated by the fact that disconnection may result in a drop in voltage and frequency. Therefore, in addition to the considerations described in the previous paragraph, droop controls need to be used to restore voltage and frequency to nominal ranges.

From the modeling standpoint, the main goal of the paper is to formulate a micro-grid optimization problem while including AC power flows to explicitly capture voltage fluctuations. To control voltage fluctuations, tap-changer, as well as droop control constraints, will be included in the formulation. Uncertainties will be captured through the use of Markov processes. The resulting problem, while generally smaller than the optimization problems solved at the main grid level, is complicated due to non-convexities caused by nonlinear AC power flows and by the discrete nature of tap changes (tap positions). Rather than using AC power flow approximations (such as DistFlow or Second-Order Cone Relaxation), an exact AC power flow in rectangular coordinates will be used.

From the methodological standpoint, the main goal of the paper is to develop an algorithm to coordinate islanded micro-grid resources at a high level while overcoming the above-mentioned difficulties, rather than to provide low-level detailed modeling of micro-grid devices. Therefore, in Section 2, important micro-grid components/features such as tap-changers, droop controls, AC power flow as well as Markovian approach for modeling uncertainties will be reviewed. Modeling of batteries and EV charging stations is out of the scope of the paper, although, the methodology to be developed in Section 3 is intended to support plug-and-play capabilities, therefore, the consideration of storage and other DERs will only affect the way subproblems are solved at the low level and will not affect the overall coordination at the high level. The gist of the "l_1-proximal" Surrogate Lagrangian Relaxation decomposition and coordination methodology is relaxation of coupling constraints (e.g., nodal flow balance) to reduce the complexity of the problem while coordinating nodal subproblems. Nonlinear constraints are linearized to both further reduce complexity and to enable the use of mixed-integer linear programming (MILP) solvers. To ensure the overall feasibility, "l_1-proximal" terms, also amenable to the use of MILP solvers, are introduced.

In Section 4, by considering a 9-bus micro-grid, the ability of the method to efficiently handle non-linearity, non-convexity, and stochasticity of the underlying problem while guaranteed feasibility is demonstrated. It is also demonstrated that the number of tap changes is drastically reduced, that the method is capable of handling networks with meshed topologies while overcoming nonlinearity difficulties brought by AC power flow, tap changer, and droop control constraints.

2. Literature Review

2.1. AC Power Flow

Because of the high r/x-ratios within distribution systems, the popular DC power flow model [1] is no longer suitable for formulating the power flows within micro-grids as well. In the following, AC Power Flow modeling methodologies will be reviewed.

1. **AC Power Flow for Radial Topologies.** The AC Power Flows are known for their non-linearity and non-convexity and the associated AC optimal power flow (AC-OPF) problem is known to be extremely difficult. One of the popular ways to handle the non-linearities is the so-called *DistFlow* model [2–6]. The model has been popular within distribution and micro-grids due to the general ease of handling linear constraints and fairly high accuracy of the approximation. The exactness of solutions, however, cannot be guaranteed. To guarantee the exactness, the model has to be nonlinear. The so-called *Second-Order Cone Relaxation* (SOCR) [7,8] addressed the exactness issue and the resulting model is convex, which is amenable for the use of commercial solvers unlike the original non-convex AC Power Flow.

 doi:10.20944/preprints202203.0389.v1

2. **AC Power Flow for Meshed Topologies.** The distribution networks (and micro-grids as their part) are not necessarily radial as acknowledged for the next generation of power distribution systems [9]. The SOCR is, however, not applicable for meshed topologies. The AC power flow in rectangular coordinates is appropriate for both radial and meshed topologies. One way to handle the associated non-convexity is by defining a convex hull of the solutions; however, even if the tightest convex relaxation is attained [10], the solution may still be inside of the convex hull rather than at its boundary, which could only be guaranteed for linear programming problems. Another approach to handle non-linearity and non-convexity is through *dynamic linearization* [11] - the linearization around the current operation point, which may change from iteration to iteration. To guarantee feasibility, the so-called "l_1-proximal" terms have been used to gradually penalize the violations of current solutions from previously obtain ones until convergence to a steady-state solution.

2.2. Droop Control

While in a grid-connected mode, micro-grids operate to control current and may inject power into the main grid, in an islanding mode, whereby microgrid is disconnected from the main grid while continuing the supply of power to local customers, micro-grid need to operate in a voltage-control mode to ensure the constant voltage to local loads. In an islanding mode, micro-grids may experience voltage fluctuations, and to recover the nominal voltage (as well as frequency), droop controls are used [12–15].

2.3. Intermittent renewables

In some studies on the operation of micro-grids, deterministic approaches were adopted, where intermittent and uncertain renewable generation is represented by its mean value without explicitly considering uncertainties. For example in [16], Photovoltaic (PV) was calculated off-line with given parameters and solar irradiation through a deterministic approach. As uncertainties are not explicitly considered, the solutions obtained by using deterministic approaches are not robust against realizations of renewable generation. To explore the intermittent and uncertain nature, stochastic programming has also been used based on representative scenarios (e.g., [17]). It is, however, difficult to select an appropriate scenario number to balance modeling accuracy, computational efficiency, and solution feasibility. To overcome the difficulties caused by scenario-based methods, a Markovian approach was developed [18]. Without considering transmission capacities, wind generation was aggregated and modeled as a Markov chain, where a state represents the wind generation at a particular hour, capturing all the past information. Since the number of states increases linearly with that of hours, the complexity is significantly reduced as compared to scenario-based methods. In our previous work [19], a Markov-based model was established to integrate intermittent and uncertain PV generation into micro-grids.

2.4. Tap-Changers

To reduce voltage deviations caused by intermittent renewables, tap changers have been used [20]. Generally, the goal is to keep the voltage amplitude within the pre-defined limits. With high levels of renewable penetration, however, to maintain power quality and reliability, transformer taps are forced to be adjusted frequently. As a result, they can rapidly reach their end of life or suffer from premature failures. As an example, Hawaii utilities reported that their on-load tap changer (OLTC) transformers, traditionally maintenance-free during a 40-year lifespan, would be maintained every three months and retire within two years because the PV-induced voltage fluctuations made the OLTC be adjusted over 300 times per day [21].

3. Micro-grid Model

Model. Consider a network with a partly-connected mesh topology operated by a micro-grid system operator (MSO). Let $\mathcal{T}$ be the planning horizon: $\mathcal{T} = \{1, 2, ..., T\}$. Let $\mathcal{B}$ be a set of buses indexed by b, $\mathcal{I}_b$ be a set of generators at bus b indexed by i, and $\mathcal{L}$ be a

Preprints (www.preprints.org) | NOT PEER-REVIEWED | Posted: 30 March 2022 doi:10.20944/preprints202203.0389.v1

sets of power lines indexed by l. Solar states are modeled by using $\mathcal{N}$ discrete states with associated probabilities $\Phi = \{\phi_{n,t}\}$ at each time period t and transition probabilities $\pi_{n,m}$ from state n to state m.

3.1. Objective

The MSO aims to minimize the total expected generation cost as well as the total expected tap-changer cost:

$$\min_{\mathbf{F},\mathbf{G},\mathbf{V},\mathbf{X}} O(\mathbf{G}) = \min_{\mathbf{F},\mathbf{G},\mathbf{V},\mathbf{X}} \left\{ \mathbf{\Phi} \cdot \mathbf{C} \cdot \mathbf{G}' + \mathbf{\Phi} \cdot \mathbf{C}^{\mathbf{tap}} \cdot \mathbf{D}' \right\}, \tag{1}$$

where $\mathbf{G} = \{g^p_{i,n,t}, g^q_{i,n,t}\}$ is a vector of active and reactive generation levels at PV state n with the corresponding generation costs $\mathbf{C} = \{C^p_{i,t}, C^q_{i,t}\}$, and $\mathbf{D} = \{d^{up}_{b,n,t}, d^{down}_{b,n,t}\}$ is a vector of the change of tap position up and down at PV state n with the corresponding tap-changing costs $\mathbf{C}^{\mathbf{tap}}$. Other decision variables include $\mathbf{X} = \{x_{i,t}\}$ - a vector of binary commitment decision variables, $\mathbf{F} = \{f^p_{l,n,t}, f^q_{l,n,t}\}$ - a vector of active (p) and reactive (q) power flows at PV state n and $\mathbf{V} = \{v^{Re}_{b,n,t}, v^{Im}_{b,n,t}\}$ - a vector of real (Re) and imaginary (Im) parts of voltages at PV state n . The optimization (1) is subject to the following constraints:

3.2. Intra-Nodal (Local) Constraints

Generation Capacity Constraints. Active and reactive generation levels are constrained as:

$$\underline{\mathbf{G}} \cdot \mathbf{X} \leq \mathbf{G} \leq \overline{\mathbf{G}} \cdot \mathbf{X}, \tag{2}$$

where $\underline{\mathbf{G}} = \{\underline{g}^p_{i,n,t}, \underline{g}^q_{i,n,t}\}$ and $\overline{\mathbf{G}} = \{\overline{g}^p_{i,t}, \overline{g}^q_{i,t}\}$ are the minimum and maximum generation levels, respectively.

Ramp-Rate Constraints. For probable transitions, ramp-rate constraints require that the change of generation levels between two consecutive time periods does not exceed ramp rates $\mathbf{R} = \{r^p_i, r^q_i\}$:

$$-\mathbf{R} \leq \mathbf{G}_{n,t} - \mathbf{G}_{m,t-1} \leq \mathbf{R}, \forall \pi_{n,m} \neq 0. \tag{3}$$

Voltage Restrictions. The voltages are subject to the following restrictions:

$$\underline{\mathbf{V}}^2 \leq \mathbf{V} \cdot \mathbf{V}' \leq \overline{\mathbf{V}}^{\mathbf{2}}, \tag{4}$$

where $\underline{\mathbf{V}}^2 = \{\underline{v_b}^2\}$ and $\overline{\mathbf{V}}^2 = \{\overline{v_b}^2\}$ with $\underline{v_b}$ and $\overline{v_b}$ being minimum and maximum voltage magnitudes.

Droop Control Constraints. It is assumed that generator $\hat{i} \in \mathcal{I}_{\hat{b}}$ employs a droop control strategy and the corresponding droop control constraints are:

$$f_{n,t} = f^{ref}_{n,t} - k_f \cdot (g^{p,ref}_{\hat{i},n,t} - g^p_{\hat{i},n,t}), \tag{5}$$

$$\sqrt{(v_{\hat{b},n,t}) \cdot (v_{\hat{b},n,t})'} = \sqrt{(v^{ref}_{\hat{b},n,t}) \cdot (v^{ref}_{\hat{b},n,t})'} - k_v \cdot (g^{q,ref}_{\hat{i},n,t} - g^q_{\hat{i},n,t}). \tag{6}$$

PV generation. Following our previous work [19], a Markov-based model is adopted for PV generation. In the model, weather uncertainties are assumed to be a Markovian process with $\mathcal{N}$ states (as a percentage of the ideal weather conditions), and state n is denoted as W_n. Based on historical data, the probability that the current weather state is n if the previous state was m can be obtained as $\pi_{m,n}$ as shown below in Figure 1.

Preprints (www.preprints.org) | NOT PEER-REVIEWED | Posted: 30 March 2022 doi:10.20944/preprints202203.0389.v1

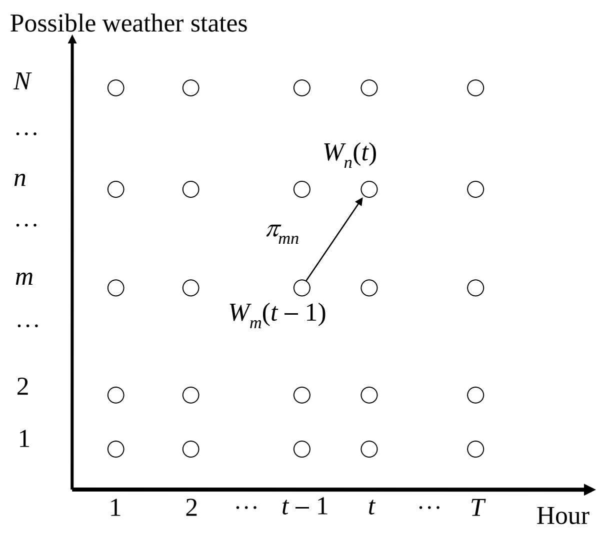

Figure 1. A Markovian process.

The uncertain PV generation $g_{n,t}^{PV}$ is also a Markovian process as follows:

$$g_{n,t}^{PV} = g_t^{IPV} W_n, \tag{7}$$

where g_t^{IPV} is the ideal PV generation at time n. The probability $\phi_{n,t}$ that the PV generation is $g_{n,t}^{PV}$ at time t is the sum of the probabilities at time $t-1$ weighted by different transitions:

$$\phi_{n,t} = \sum_{m=1..N} \pi_{n,m} \phi_{n,t-1}. \tag{8}$$

The probabilities of PV generation levels for future time slots can be obtained based on the initial PV generation state and the transition matrix.
Tap changer. Assume that there is one tap changer associated with one solar farm, and the bus index is omitted for brevity. Following [20], tap changer constraints can be written as:

$$V_{n,t} = \frac{1}{a_{n,t}} V^{in} - \frac{a_{n,t} Z_{t(a)} S_n}{(V^{in})^*}, \tag{9}$$

where V^{in} is the input voltage and V_n is a decision variable, a is the transformer turn ratio defined under no load conditions as: V^{in}/V_n, $Z_{t(a)}$ is transformer leakage impedance, which generally is a function of a, but in this paper it is assumed that $Z_{t(a)}$ is a complex number, and S is the transformer load. Equation (9) can be equivalently written as:

$$a_{n,t}(V^{in})^* V_n = V^{in}(V^{in})^* + (a_{n,t})^2 Z_{t(a)} S_n. \tag{10}$$

The transformer turn ratios $a_{n,t}$, which are decision variables, are controlled as:

$$a_{n,t} = a_0 + d_{n,t} \Delta a, \tag{11}$$

where a_0 is the rated turn ratio (usually 1), Δa is the single tap position change, and $\{d_{n,t}\}$ are integer decision variables denoting tap positions as:

$$d_{n,t} = d_{n,t-1} + d_{n,t}^{up} - d_{n,t}^{down}. \tag{12}$$

3.3. Inter-Nodal (Global) Constraints

AC Power Flow Constraints in Rectangular Coordinates. Following [22–26], AC power flow is modeled in rectangular coordinates by using complex voltages $v_{b,n,t} = v_{b,n,t}^{Re} + j \cdot$

Preprints (www.preprints.org) | NOT PEER-REVIEWED | Posted: 30 March 2022 doi:10.20944/preprints202203.0389.v1

$v^{Im}_{b,n,t}$. In the complex plane, complex voltages can be represented as row vectors $v_{b,n,t} = \left(v^{Re}_{b,n,t}, v^{Im}_{b,n,t}\right)$ and power flows can be compactly written as:

$$f^p_{l,n,t} = v_{s(l),n,t} \cdot \begin{pmatrix} g_{s(l),r(l)} & \text{-}b_{s(l),r(l)} \\ b_{s(l),r(l)} & g_{s(l),r(l)} \end{pmatrix} \cdot \left(v_{r(l),n,t}\right)', \tag{13}$$

$$f^q_{l,n,t} = v_{s(l),n,t} \cdot \begin{pmatrix} \text{-}b_{s(l),r(l)} & \text{-}g_{s(l),r(l)} \\ g_{s(l),r(l)} & \text{-}b_{s(l),r(l)} \end{pmatrix} \cdot \left(v_{r(l),n,t}\right)'. \tag{14}$$

Here $b_{s(l),r(l)}$ is susceptance and $g_{s(l),r(l)}$ is conductance of line $(s(l), r(l))$. Node $s(l)$ denotes the "sending" node of line l, and $r(l)$ denotes the "receiving" node of the line l.
Nodal Power Flow Balance Constraints. For every PV state n at every node b, the net active/reactive power generated and transmitted to the node should be equal to the net power consumed and transmitted from node b:

$$\sum_{i \in \mathcal{I}_b} g^p_{i,n,t} + g^{PV,p}_{b,n,t} + \sum_{\substack{l=1: \\ r(l)=b}}^{L} f^p_{l,n,t} = L^p_{b,t} + \sum_{\substack{l=1: \\ s(l)=b}}^{L} f^p_{l,n,t}, \tag{15}$$

$$\sum_{i \in \mathcal{I}_b} g^q_{i,n,t} + g^{PV,q}_{b,n,t} + \sum_{\substack{l=1: \\ r(l)=b}}^{L} f^q_{l,n,t} = L^q_{b,t} + \sum_{\substack{l=1: \\ s(l)=b}}^{L} f^q_{l,n,t}. \tag{16}$$

If bus b does not contain generators, then $\sum_{i \in \mathcal{I}_b} g^{p/q}_{i,n,t} = 0$, if bus b does not contain load, then $L^{p/q}_{b,t} = 0$, and if there is no PV generation, then $g^{PV,p/q}_{b,n,t} = 0$
Line Capacity Constraints. Power flows in each line l at each PV state n satisfy the following line capacity constraints:

$$\sqrt{\left(f^p_{l,n,t}\right)^2 + \left(f^q_{l,n,t}\right)^2} \leq \overline{f}_l. \tag{17}$$

The above problem belongs to a class of Mixed-Integer Nonlinear Programming problems notable for non-convexities brought by nonlinear AC power flows as well as by discrete decision variables.

4. Solution Methodology

To resolve the above difficulties, a solution methodology is developed based on the recent "l_1- proximal" Surrogate Lagrangian Relaxation method [11]. The main ideas behind the method are linearization of resulting subproblems, coordination of subproblem solutions through the update of Lagrangian multipliers, and penalization of constraint violations as well as "l_1- proximal" terms to ensure feasibility.

4.1. Surrogate Absolute-Value Lagrangian Relaxation

Relaxed Problem. After relaxing nodal flow balance (15)-(16), and penalizing their violations, the relaxed problem becomes:

$$\min_{\mathbf{F},\mathbf{G},\mathbf{V},\mathbf{X}} L_c(\mathbf{G}; \mathbf{\Lambda}) = \min_{\mathbf{F},\mathbf{G},\mathbf{V},\mathbf{X}} \left\{ O(\mathbf{G}) + \mathbf{\Lambda} \cdot \mathbf{R} + c \cdot \left\|\mathbf{R}\right\|_1 \right\}, s.t., (2) - (14), (17),$$

where $\mathbf{\Lambda}_j = \left(\mathbf{\Lambda}^P_j, \mathbf{\Lambda}^Q_j\right)$ are multipliers relaxing active/reactive power flow balance constraints (16). The vector, $\mathbf{R} = \left(\mathbf{B}^P, \mathbf{B}^Q\right)'$ denotes a vector of active/reactive power flow balance constraint violations.
Multiplier Update. The multipliers are updated as follows:

$$\mathbf{\Lambda}^k = \mathbf{\Lambda}^{k-1} + s^k \cdot \mathbf{R}^k. \tag{18}$$

Stepsize Update. Following [11], the stepsize is updated in the following way:

$$s^k = \alpha^k \cdot s^{k-1} \cdot \frac{\left\|\mathbf{R}^{k-1}\right\|_2}{\left\|\mathbf{R}^k\right\|_2}, \tag{19}$$

where α^k is a step-sizing parameter

$$\alpha^k = 1 - \frac{1}{M \cdot k^{1-\frac{1}{k^r}}}, M > 1, r > 0. \tag{20}$$

Penalty Coefficient Update. In the beginning of the iterative process, the penalty coefficient c^k increases by a predetermined constant $\beta > 1$:

$$c^k = c^{k-1} \cdot \beta. \tag{21}$$

The intent is to increase the value of c^k until the norm of constraint violations reduces to zero and a feasible solution is obtained, after which the penalty coefficient is decreased per

$$c^k = c^{k-1} \cdot \beta^{-1} \tag{22}$$

Subsequently, the penalty coefficient is not increased.

4.2. Practical Considerations of the Method

In practical implementations, the following considerations are important. Voltage restrictions (4), droop control for voltage (6), tap-changer constraints (10), AC power flows (13)-(14), as well as line capacity constraints (17) are nonlinear, they need to be appropriately linearized while maintaining feasibility. Moreover, the left-hand side constraint of (4) and (13)-(14) delineate non-convex regions. Following the work [11], the considerations are briefly addressed next. The method of [11] is then extended to improve the linearization of (4) as well as to resolve non-linearity difficulties brought by the newly considered droop control (6) and tap-changer constraints (10).

In the following, the main linearization principles will be delineated first. Then, the feasibility will be established.

1. **Linearization of Cross-Product Terms within** (13)**-**(14)**.** To linearize AC Power Flow while updating all the voltages, the following formula is used:

$$\widehat{f}^p_{l,t} = \frac{1}{2} v^{k-1}_{s(l),t} \cdot \begin{pmatrix} g_{s(l),r(l)} & \text{-}b_{s(l),r(l)} \\ b_{s(l),r(l)} & g_{s(l),r(l)} \end{pmatrix} \cdot \left(v_{r(l),t}\right) + \frac{1}{2} v_{s(l),t} \cdot \begin{pmatrix} g_{s(l),r(l)} & \text{-}b_{s(l),r(l)} \\ b_{s(l),r(l)} & g_{s(l),r(l)} \end{pmatrix} \cdot \left(v^{k-1}_{r(l),t}\right). \tag{23}$$

Reactive power flows are linearized in the same way.

2. **Linearization of Voltage Restrictions** (4). First, the squared terms within (4) are then linearized in the following way:

$$\underline{\mathbf{V}}^2 \leq \mathbf{V}^{k-1} \cdot \mathbf{V}' \leq \overline{\mathbf{V}}^{\mathbf{2}}. \tag{24}$$

To avoid infeasibility along the iterative procedure, "soft" penalization in introduced through the non-negative penalty variables $\underline{\mathbf{V}}^{pen} = \{\underline{v}^{pen}_{b,t}\}$ and $\overline{\mathbf{V}}^{pen} = \{\overline{v}^{pen}_{b,t}\}$ as:

$$\underline{\mathbf{V}}^2 - \underline{\mathbf{V}}^{pen} \leq \mathbf{V}^{k-1} \cdot \mathbf{V}' \leq \overline{\mathbf{V}}^{\mathbf{2}} + \overline{\mathbf{V}}^{\mathbf{pen}}. \tag{25}$$

To enforce feasibility of (25), $\underline{\mathbf{V}}^{pen}$ and $\overline{\mathbf{V}}^{pen}$ are penalized.

Preprints (www.preprints.org) | NOT PEER-REVIEWED | Posted: 30 March 2022 doi:10.20944/preprints202203.0389.v1

3. **Linearization of Tap-Changer Constraints** (10). Tap-changer constraints contain both, the cross-products and the squared terms. Following the ideas of above-presented linearization, the linearization is performed as follows:

$$\frac{1}{2}a_{n,t}^{k-1}(V^{in})^* V_n + \frac{1}{2}a_{n,t}(V^{in})^* V_n^{k-1} = V^{in}(V^{in})^* + a_{n,t}^{k-1}a_{n,t}Z_{t(a)}S_n. \quad (26)$$

The linearization of voltage droop control constraints (6) as well as line capacity constraints (17) is operationalized in the same way as described in point 2 and 3 above. To ensure that solutions satisfying constraints (23), (25) and (26) satisfy the corresponding original constraints (13), (4) and (10), respectively, proximal-like terms $\|\mathbf{V} - \mathbf{V}^{k-1}\|_1$, $\|\widehat{\mathbf{F}} - \widehat{\mathbf{F}}^{k-1}\|_1$, and $\|\mathbf{A} - \mathbf{A}^{k-1}\|_1$, which capture the deviations of voltages $\mathbf{V}$, linearized power flows $\widehat{\mathbf{F}}$ and transformer turns ratios $\mathbf{A} \equiv \{a_{n,t}\}$ from previously obtained values are introduced and penalized by c_p^k. The intention here is to discourage oscillations of solutions while encouraging their approach to common values through a separate penalty coefficient, lower in value as compared to c^k, is to avoid solutions getting trapped at previously obtained values.

Linearized Relaxed Problem. The resulting MSO relaxed problem then becomes:

$$\min_{\mathbf{A},\widehat{\mathbf{F}},\mathbf{G},\mathbf{V},\mathbf{X}} \left\{ \begin{array}{l} L_{c^{k-1}}(\mathbf{G};\mathbf{\Lambda}^{k-1}) + c_p^{k-1}\left(\|\mathbf{V}-\mathbf{V}^{k-1}\|_1 + \|\widehat{\mathbf{F}}-\widehat{\mathbf{F}}^{k-1}\|_1 + \|\mathbf{A}-\mathbf{A}^{k-1}\|_1\right) + \\ \underline{\mathbf{\Lambda}}^{pen}\cdot\left(\underline{\mathbf{V}}^2-\mathbf{V}^{k-1}\cdot\mathbf{V}'\right) + \overline{\mathbf{\Lambda}}^{pen}\cdot\left(\mathbf{V}^{k-1}\cdot\mathbf{V}'-\overline{\mathbf{V}}^{\mathbf{2}}\right) + c^{k-1}\cdot\underline{\mathbf{V}}^{pen} + c^{k-1}\cdot\overline{\mathbf{V}}^{pen} \end{array} \right\}, \quad (27)$$

$s.t.$, (2) − (3), (5), (11) − (12), (15) − (16), (23), (25) − (26).

The multiplier update for (27) is operationalized by appending constraints violations $\mathbf{R}$ by $\left(\underline{\mathbf{V}}^2-\mathbf{V}^{k-1}\cdot\mathbf{V}'\right)$ and $\left(\mathbf{V}^{k-1}\cdot\mathbf{V}'-\overline{\mathbf{V}}^{\mathbf{2}}\right)$, and multipliers $\mathbf{\Lambda}$ by $\underline{\mathbf{\Lambda}}^{pen}$ and $\overline{\mathbf{\Lambda}}^{pen}$, and by following the multiplier updating procedure described in (18) with projections of negative values of $\underline{\mathbf{\Lambda}}^{pen}$ and $\overline{\mathbf{\Lambda}}^{pen}$ onto a positive orthant $\{\lambda|\lambda \geq 0\}$. Piece-wise linear l_1-norms within (27) are linearized following standard procedures [27,28].

Feasibility. As penalty coefficients c^k increase, violation levels of relaxed constraints decrease. However, the total lack of constraint violations does not imply feasibility because, for example, linearized power flows do not coincide with original power flows. To ensure that $\widehat{f}_{l,t}^p \to f_{l,t}^p$ and $\widehat{f}_{l,t}^q \to f_{l,t}^q$, penalty coefficients c_p^k increase in a manner similar to (21) as:

$$c_p^k = c_p^{k-1} \cdot \beta_p. \quad (28)$$

The intent is to increase the value of c_p^k until the "l_1-proximal" terms reduce to zero and a feasible solution is obtained, after which the penalty coefficient is decreased per

$$c_p^k = c_p^{k-1} \cdot \beta_p^{-1}. \quad (29)$$

After constraints violations become zero, the feasible solution is obtained. After the reduction of penalty coefficients, multipliers are updated again until constraint violations and proximal terms are zero again, and the process repeats. The reduction of constraint violations and proximal terms to exactly zero may require significant CPU time, so the algorithm stops when constraint violations are less than a predetermined value ϵ and proximal terms are less than ϵ_p.

4.3. Algorithm.

Stopping Criteria. Within the above Algorithm, the "if" condition in step **4** can by itself be used as a stopping criterion. Alternatively, after c is reduced per **4**, the algorithm can continue with the multipliers update until a predefined CPU limit us reached.

Preprints (www.preprints.org) | NOT PEER-REVIEWED | Posted: 30 March 2022 doi:10.20944/preprints202203.0389.v1

Algorithm 1 Surrogate Lagrangian Relaxation

Initialize $\mathbf{\Lambda}^0$, c^0, c_p^0 and s^0
while stopping criteria are not satisfied
1 solve MSO problem
2 If the total constraints violations $> \epsilon$ and total violation of proximal terms is $> \epsilon_p$ update multipliers and increase c
3 If the total constraints violations $< \epsilon$ and total violation of proximal terms is $> \epsilon_p$ update multipliers, stop increasing c and increase c_p
4 If the total constraints violations $< \epsilon$ and total violation of proximal terms is $< \epsilon_p$ reduce c and stop increasing c_p.

5. Results

The method is implemented using IBM ILOG CPLEX Optimization Studio V 12.8.0.0 [29] on a PC with 2.40GHz Intel Xeon E-2286M CPU and 32G RAM. To demonstrate the coordination aspect and the near-optimal performance of the method, a simple 9-bus system is considered.

5.1. System description

Consider a 9 bus system with meshed topology as shown in Figure 2. below [30]. Assume that at buses 2 and 3 there is a generator, respectively, at bus 4 there is a solar farm of three stochastic states, and a tap changer, while at buses 5, 7, and 9, there is load. The micro-grid is connected to the main grid through bus 1. The time interval is 15 minutes and the planning horizon is 3 hours.

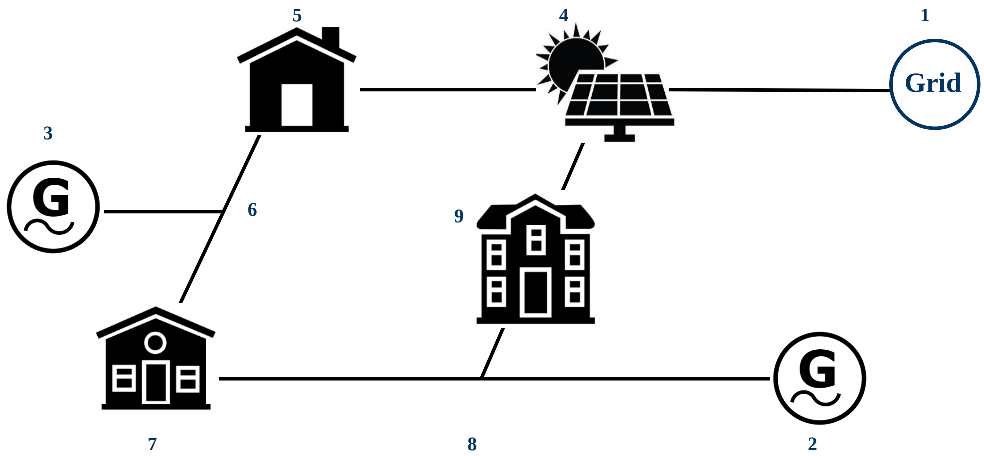

Figure 2. Topology of the 9-bus system.

5.2. Results and discussions

5.2.1. Droop control

To demonstrate the performance of droop control, the micro-grid is disconnected from the grid at interval 12; thus, turning the local operations into the islanded mode. By using the approach developed above, the problem (1)-(17) is solved, and a feasible solution is obtained in 202 seconds. The results show that the frequency stays within the range of [59 Hz, 61 Hz] due to effective droop control.

5.2.2. Tap-changer

To show the impacts of tap changing, the problem in 5.2.1 is solved again without tap-change-related costs in the objective function. The results are compared in Table 1 below. It can be seen that the expected number of tap changes is much reduced when the corresponding cost is considered in the objective function.

Preprints (www.preprints.org) | NOT PEER-REVIEWED | Posted: 30 March 2022 doi:10.20944/preprints202203.0389.v1

Table 1. Results on tap-changing

	Expected number of tap changes	Solving time
Without tap-changing cost	7	202 sec
With tap-changing cost	0	262 sec

5.2.3. Costs

To show the benefits of being connected to the main grid all the time, the problem in 5.2.1 is solved again under the grid-connected mode. The results are compared in Table 2 below. It can be seen that the total cost is reduced by connecting to the main grid, taking advantage of the time-vary costs of the grid power.

Table 2. Results of two different grid-connection scenarios

	Expected cost	Expected number of tap changes	Solving time
Grid connected until interval 11	$37,126	0	202 sec
Grid connected all the time	$36,724	0	154 sec

6. Conclusions

In anticipation of the transition of the fully centralized operations toward more distributed generation supported by the emergence of micro-grids, this paper addresses the issues of sustainability of the micro-grid operations: through the consideration of Markov processes to capture stochasticity of the renewable generation; through tap-changer constraints penalizing frequent changes of taps, the lifespan of the expensive equipment will be greatly extended; through consideration of AC power flow constraints appropriate for distribution systems; through droop-control constraints for restoration of frequency and voltage after the disconnection from the main grid. The abovementioned constraints lead to non-convexities and the difficulties of solving the resulting micro-grid operation optimization problems. The methodology based on dynamic linearization and l_1-norm penalization is exact and is amenable for the use of MILP solvers. It is also demonstrated that the micro-grids' operations benefit from the new solution methodology, specifically, AC power flows are satisfied exactly ensuring the feasibility of operations and the number of tap changes is drastically reduced thereby ensuring higher sustainability in the presence of voltage fluctuations caused by uncertainties.

Author Contributions: Conceptualization, P.Z.; methodology, M.A.B., and B.Y.; software, M.A.B., B.Y. and A.K.; validation, B.Y., and A.K.; investigation, M.A.B.; data curation, B.Y.; writing—original draft preparation, M.A.B., B.Y., A.K. and N.Y.; writing—review and editing, M.A.B., B.Y., A.K. and N.Y.; visualization, M.A.B., B.Y.; supervision, P.Z.; project administration, P.Z., N.Y., M.A.B.; funding acquisition, P.Z., M.A.B., and B.Y. All authors have read and agreed to the published version of the manuscript.

Funding: This work is supported in part by the National Science Foundation under the grant ECCS-1810108, CNS- 2006828 and OIA- 2134840.

Abbreviations

The following abbreviations are used in this manuscript:

MILP	Mixed-Integer Linear Programming
MSO	Micro-grid system operator
OLTC	on-load tap changer
OPF	Optimal Power Flow
PV	Photovoltaic
SOCR	Second-Order Cone Relaxation

References

1. B. Stott, J. Jardim, and O. Alsac, "DC power flow revisited," IEEE Trans. Power Syst., vol. 24, no. 3 pp. 1290–1300, Aug. 2009.
2. H. G. Yeh, D. F. Gayme, S. H. Low, Adaptive var control for distribution circuits with photovoltaic generators, IEEE Transactions on Power Systems 27 (3) (2012) 1656–1663.
3. S. Tan, J. Xu, S. K. Panda, Optimization of distribution network incorporating distributed generators: An integrated approach, IEEE Transactions on Power Systems 28 (3) (2013) 2421–2432.
4. M. Farivar, S. H. Low, Branch flow model: Relaxations and convexification—Part I, IEEE Transactions on Power Systems 28 (3) (2013) 2554–2564.
5. G. Liu, T. Jiang, T. B. Ollis, X. Zhang, K. Tomsovic, Distributed energy management for community microgrids considering network operational constraints and building thermal dynamics, Applied energy 239 (2019) 83–95.
6. Z. Wang, H. Chen, J. Wang, M. Begovic, Inverter-less hybrid voltage/var control for distribution circuits with photovoltaic generators, IEEE Transactions on Smart Grid 5 (6) (2014) 2718–2728.
7. S. S. Torbaghan, G. Suryanarayana, H. Höschle, R. D'hulst, F. Geth, C. Caerts, and D. Van Hertem, "Optimal Flexibility Dispatch Problem Using Second-Order Cone Relaxation of AC Power Flows," *IEEE Transactions on Power Systems*, vol. 35, No. 1, pp. 98-108, 2020.
8. M. Farivar and S. H. Low, "Branch Flow Model: Relaxations and Convexification - Part I," *IEEE Transactions on Power Systems*, vol. 28, no. 3, pp. 2554-2564, Aug. 2013.
9. G. Heydt, "The next generation of power distribution systems," IEEE Trans. Smart Grid, vol. 1, no. 3, pp. 225–235, Dec. 2010.
10. Q. Li and V. Vittal, "The convex hull of the AC power flow equations in rectangular coordinates," in Proc. IEEE Power & Energy Soc. General Meeting, Boston, MA, USA, Jul. 2016, pp. 1–5.
11. M. A. Bragin, and Y. Dvorkin, "TSO-DSO Operational Planning Coordination through "l_1-Proximal" Surrogate Lagrangian Relaxation," Early Access, IEEE Transactions on Power Systems. DOI: 10.1109/TPWRS.2021.3101220.
12. A. Maulik, D. Das, Optimal operation of droop-controlled islanded microgrids, IEEE Transactions on Sustainable Energy 9 (3) (2017) 1337–1348.
13. B. Alghamdi, C. A. Canizares, Frequency regulation in isolated microgrids through optimal droop gain and voltage control, IEEE Transactions on Smart Grid 12 (2) (2020) 988–998.
14. W. T. Elsayed, H. Farag, H. H. Zeineldin, E. F. El-Saadany, Formation of islanded droop-based microgrids with optimum loadability, IEEE Transactions on Power Systems (2021).
15. R. A. Jabr, Mixed-integer convex optimization for dc microgrid droop control, IEEE Transactions on Power Systems (2021).
16. X. Guan, Z. Xu, and Q. Jia, "Energy-efficient buildings facilitated by microgrid," *IEEE Transactions on Smart Grid*, Vol. 1, Issue 3, pp. 243-252, 2010.
17. S. Mohammadi, S. Soleymani, and B. Mozafari, "Scenario-based stochastic operation management of MicroGrid including Wind, Photovoltaic, Micro-Turbine, Fuel Cell and Energy Storage Devices," *Electrical Power and Energy Systems*, Vol. 54, pp. 1-7, 2014.
18. P. B. Luh, Y. Yu, B. Zhang, E. Litvinov, T. Zheng, F. Zhao, J. Zhao, and C. Wang, "Grid integration of intermittent wind generation: a Markovian approach," *IEEE Transactions on Smart Grid*, Vol. 5, Issue 2, pp. 732-741, 2014.
19. B. Yan, P. B. Luh, G. Warner, and P. Zhang, "Operation Optimization for Microgrids with Renewables," *IEEE Transactions on Automation Science and Engineering*, Vol. 14, Issue 2, pp. 573 - 585, 2017.
20. B. Kasztenny, E. Rosolowski, J. Izykowski, M M. Saha, and B. Hillstrom, "Fuzzy logic controller for on-load transformer tap changer," *IEEE Transactions on Power Delivery*, Vol 13, no. 1, pp. 164-170, 1998.
21. T. Sokugawa and M. Shawver, "Big data for renewable integration at Hawaiian electric utilities," in Proceedings of DistribuTech Conference & Exhibition, Orlando, FL, pp. 9-11, 2016.
22. G. L. Torres, V. H. Quintana, and G. Lambert-Torres, "Optimal Power Flow on Rectangular Form Via an Interior Point Method," *in IEEE North American Power Symposium*, 1996.
23. V. da Costa, N. Martins, and J. L. R. Pereira, "Developments in the Newton Raphson Power Flow Formulation Based on Current Injections," *IEEE Transactions on Power Systems*, vol. 14, no. 4, pp. 1320–1326, November 1999.
24. X. P. Zhang, S. G. Petoussis, and K. R. Godfrey, "Nonlinear Interior Point Optimal Power Flow Method Based on a Current Mismatch Formulation," *IEEE Proceedings-Generation, Transmission and Distribution*, vol. 152, no. 6, pp. 795–805, November 2005.
25. X. Bai, H.Wei, K. Fujisawa, and Y.Wang, "Semidefinite Programming for Optimal Power Flow problems," *International Journal of Electrical Power and Energy Systems*, vol. 30, no. 6-7, pp. 383-392, 2008.
26. Q. Li , L. Yang and S. Lin, "Coordination Strategy for Decentralized Reactive Power Optimization Based on a Probing Mechanism," *IEEE Transactions on Power Systems*, vol. 30, no. 2, pp. 555-562, Mar. 2015.

27. M. A. Bragin, P. B. Luh, B. Yan, and X. Sun, "A Scalable Solution Methodology for Mixed-Integer Linear Programming Problems Arising in Automation," IEEE Transaction on Automation Science and Engineering, vol. 16, issue 2, April 2019, pp. 531-541. DOI: 10.1109/TASE.2018.2835298. (2020 Best Transactions Paper Honorable Mention)
28. X. Sun, P. B. Luh, M. A. Bragin, Y. Chen, J. Wan, and F. Wang, "A Novel Decomposition and Coordination Approach for Large-Scale Security Constrained Unit Commitment Problems with Combined Cycle Units," IEEE Transactions on Power Systems, vol. 33, issue 5, Sept. 2018, pp. 5297-5308. DOI: 10.1109/PESGM.2017.8274098.
29. IBM ILG CPLEX V 12.1 User's Manual.
30. R. D. Zimmerman, C. E. Murillo-Sanchez (2020). MATPOWER (Version 7.1) [Software]. Available: https://matpower.org.